

Neutral Hexacoordinate Silicon Tris-Chelates: Structure and Stereodynamics[†]

Inna Kalikhman,* Vijeyakumar Kingston, Olga Girshberg, and Daniel Kost*

Department of Chemistry, Ben-Gurion University of the Negev, Beer-Sheva 84105, Israel

Received June 4, 2001

Neutral hexacoordinate silicon chelates with two chloro ligands (**1**) have been converted to neutral tris-chelates (**6** and **7**) by reaction with bis-(*O,O*-trimethylsilyl)catechol (**4**) and (*Z*)-Me₃SiO(Ph)C=NNHSiMe₃ (**5**), respectively. Likewise, zwitterionic dichloro-hexacoordinate chelate (**2a**) was converted to the zwitterionic tris-chelate **8** with three different chelate rings, by reaction with **4**. 2D-NOESY NMR spectra at various temperatures for **6a** and **7a** and for the chirally labeled **6b** and **7c** showed two consecutive ligand-site exchange processes, assigned to interchange of dimethylhydrazido-chelate rings via (O,O)-1,2-shift (**6a**, $\Delta G^* = 20.8 \text{ kcal mol}^{-1}$, **7a**, $18.5 \text{ kcal mol}^{-1}$) and dissociation–recombination of the N–Si bond. In **8**, the NMR evidence shows that the *lower* process is N–Si dissociation–recombination, followed by enantiomerization at silicon via (O,O)-exchange ($\Delta G^* = 16.1$ and $20.9 \text{ kcal mol}^{-1}$, respectively).

The chemistry of hexacoordinate silicon complexes has attracted considerable attention in recent years.¹ We have previously described convenient methods for the preparation of neutral² and zwitterionic³ octahedral silicon bis-chelates. Both methods led to formation of several hexacoordinate *dichloro*-bis-chelates (**1**, **2**), which might be used as starting materials for further ligand substitution leading to novel silicon complexes, including tris-chelates of neutral hexacoordinate silicon. A few *ionic* silicon tris-chelates have been described previously,⁴ and only a handful of neutral silicon tris-chelates have been published.⁵ Very little is known on the stereodynamic behavior of these chelates: whether they undergo ligand-site exchange reactions, and whether these are intramolecular or involve dissociation of bonds.¹ Previous studies have shown intricate ligand-

exchange mechanisms in neutral hexacoordinate silicon bis-chelates.^{2b–d}

We report on the preparation, characterization, and stereodynamic behavior of three types of new neutral tris-chelates of hexacoordinate silicon (**6**–**8**). One of these, **8**, is the first reported case of a silicon chelate with three different chelate rings.

Results and Discussion

Synthesis and Structure. When dichloro complexes **1a–c** reacted with bis-trimethylsilyl-bidentate ligands **4** and **5**, ligand exchange with evolution of Me₃SiCl (**3**) took place, forming the tris-chelates **6a,b** and **7a,c** in 60–80% yields (eq 1). Similarly, the reaction of the zwitterionic dichloro-bis-chelate **2a** with **4** led to the novel zwitterionic tris-chelate (**8**), with *three different chelate rings* (eq 2). Tris-chelates **6a**, **7a**, and **8** were subjected to single-crystal structural analysis, and their molecular structures in the crystal are presented in Figures 1–3 and in Table 1. In all three chelates the silicon coordination spheres are close to octahedral

[†] Dedicated to Professor Mikhail Voronkov on the occasion of his 80th birthday.

(1) For reviews on hypervalent silicon compounds see: (a) Chuit, C.; Corriu, R. J. P.; Reyé, C. In *The Chemistry of Hypervalent Compounds*; Kin-ya Akiba, Ed.; Wiley-VCH: Chichester, U.K., 1999; p 81. (b) Kost, D.; Kalikhman, I. In *The Chemistry of Organic Silicon Compounds*; Apeloig, Y., Rappoport, Z., Eds.; Wiley, Chichester, U.K., 1998; Vol. 2, p 1339. (c) Holmes, R. R. *Chem. Rev.* **1990**, *90*, 17; **1996**, *96*, 927. (d) Lukevics, E.; Pudova, O. A. *Khim. Geterotsiklicheskikh Soedin.* **1996**, 1605; *Chem. Abstr.* **1997**, *126*, 157528w. (e) Corriu, R. J. P.; Young, J. C. In *The Chemistry of Organic Silicon Compounds*; Patai, S., Rappoport, Z., Eds.; Wiley: Chichester U.K., 1989; p 1241. (f) Chuit, C.; Corriu, R. J. P.; Reyé, C.; Young, J. C. *Chem. Rev.* **1993**, *93*, 1371. (g) Tandura, St. N.; Alekseev, N. V.; Voronkov, M. G. *Top. Curr. Chem.* **1986**, *131*, 99. (h) Tacke, R.; Pülm, M.; Wagner, B. *Adv. Organomet. Chem.* **1999**, *44*, 221.

(2) (a) Mozzhukhin, A. O.; Antipin, M. Yu.; Struchkov, Yu. T.; Gostevskii, B. A.; Kalikhman, I. D.; Pestunovich, V. A.; Voronkov, M. G. *Metallorg. Khim.* **1992**, *5*, 658; *Chem. Abstr.* **1992**, *117*, 234095w. (b) Kost, D.; Kalikhman, I.; Raban, M. *J. Am. Chem. Soc.* **1995**, *117*, 11512. (c) Kost, D.; Kalikhman, I.; Krivonos, S.; Stalke, D.; Kottke, T. *J. Am. Chem. Soc.* **1998**, *120*, 4209. (d) Kost, D.; Krivonos, S.; Kalikhman, I. In *Organosilicon Chemistry III*; Auner, N., Weis, J., Eds.; VCH: Weinheim, 1997; pp 435–445. (e) Kalikhman, I.; Krivonos, S.; Stalke, D.; Kottke, T.; Kost, D. *Organometallics* **1997**, *16*, 3255.

(3) Kalikhman, I.; Girshberg, O.; Lameyer, L.; Stalke, D.; Kost, D. *Organometallics* **2000**, *19*, 1927.

(4) (a) Carré, F.; Cerveau, G.; Chuit, C.; Corriu, R. J. P.; Reyé, C. *Angew. Chem., Int. Ed. Engl.* **1989**, *28*, 489. (b) Carré, F.; Chuit, C.; Corriu, R. J. P.; Mehdi, A.; Reyé, C. *J. Organomet. Chem.* **1993**, *446*, C6. (c) Carré, F.; Chuit, C.; Corriu, R. J. P.; Fanta, A.; Mehdi, A.; Reyé, C. *Organometallics* **1995**, *14*, 194. (d) Chuit, C.; Corriu, R. J. P.; Mehdi, A.; Reyé, C. *Chem. Eur. J.* **1996**, *2*, 342. (e) Kummer, D.; Köster, H. Z. *Anorg. Allg. Chem.* **1973**, *402*, 297. (f) Kummer, D.; Gaisser, K. E.; Seifert, J.; Wagner, R. Z. *Anorg. Allg. Chem.* **1979**, *459*, 145. (g) Flynn, J. J.; Boer, F. P. *J. Am. Chem. Soc.* **1969**, *91*, 5756. (h) Hoppe, M. L.; Laine, M.; Kampf, J.; Gordon, M. S.; Burggraf, L. W. *Angew. Chem., Int. Ed. Engl.* **1993**, *32*, 287. (i) Tacke, R.; Willeke, M.; Penka, M. Z. *Anorg. Allg. Chem.* **2001**, *627*, 1236. (j) Tacke, R.; Stewart, A.; Becht, J.; Burschka, C.; Richter, I. *Can. J. Chem.* **2000**, *78*, 1380. (k) Kira, M.; Zhang, L. C.; Kabuto, C.; Sakurai, H. *Organometallics* **1998**, *17*, 887.

(5) (a) Farnham, W. B.; Whitney, J. F. *J. Am. Chem. Soc.* **1984**, *106*, 3992. (b) Carré, F.; Cerveau, G.; Chuit, C.; Corriu, R. J. P.; Reyé, C. *New J. Chem.* **1992**, *16*, 63. (c) Karsch, H. H.; Richter, R.; Witt, E. *J. Organomet. Chem.* **1996**, *521*, 185.

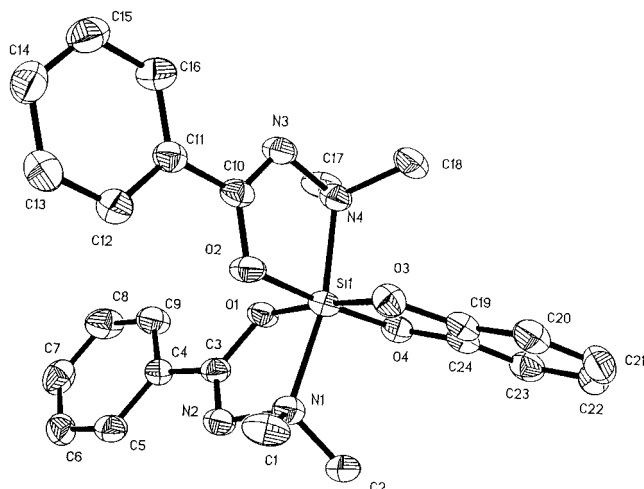
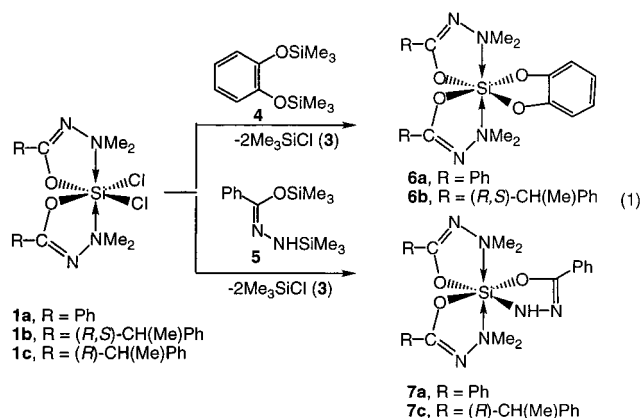
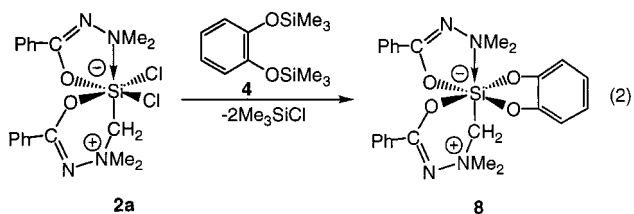


Figure 1. Molecular structure in the crystal of **6a**. The ellipsoids correspond to a 50% probability level. Hydrogen atoms have been omitted for clarity.



geometries, with the least symmetric molecule (**8**, with three different chelate rings) being nearest to a true octahedral structure.



It is interesting to note that substitution of the chloro ligands in all three cases preserved the chelate disposition of the initial dichloro compounds;^{2c,3} the nitrogen atoms of the first two chelate rings in **6** and **7** and the nitrogen and carbon atoms in **8** remained in trans position, while the oxygen atoms in the initial chelate rings in **1** and **2** retained their cis arrangement in the products **6–8**. It follows that in these reactions ligand displacement between different silicon fragments takes place with retention of the initial geometry about silicon.

The structures of **6–8** in solution generally conform to the crystal structures, as concluded from the ²⁹Si chemical shifts (Table 2): on one hand, the shifts fall well within the range for hexacoordinate complexes, but on the other hand the resonances are shifted somewhat relative to the dichloro starting materials [$\delta^{29}\text{Si}$ of

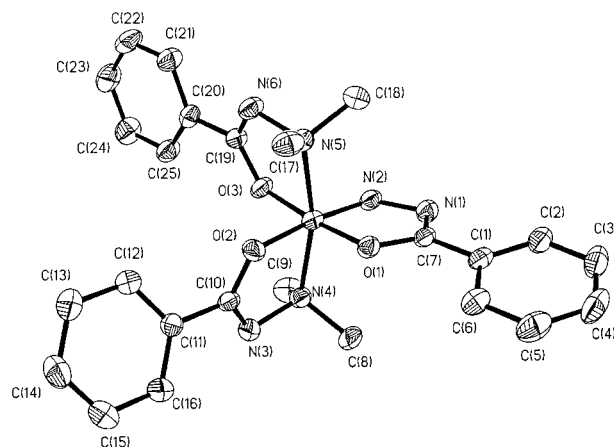


Figure 2. Molecular structure in the crystal of **7a**. The ellipsoids correspond to a 50% probability level. Hydrogen atoms have been omitted for clarity.

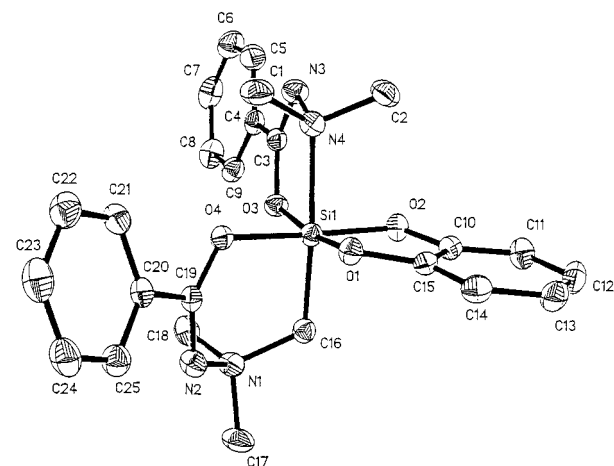


Figure 3. Molecular structure in the crystal of **8**. The ellipsoids correspond to a 50% probability level. Hydrogen atoms have been omitted for clarity.

1a = -145.9 ; **1b** = -146.1 , -146.4 , -146.6 (three diastereomers); **1c** = -146.2 , -146.8 (two diastereomers); **2a** = -158.8 ppm].

Ligand-Site Exchange in 6a,b. Since hexacoordinate silicon complexes have been shown in many studies^{1a–c,e–f,2} to undergo multistep intramolecular stereomutations, observable by variable-temperature NMR spectroscopy, it was of interest to investigate the ligand exchange phenomena in tris-chelates **6–8**. In particular, the question whether the N–Si bond does or does not dissociate during ligand-site exchange reactions was asked.

We begin with the C_2 symmetric tris-chelate, **6a**. Due to symmetry, only two signals for the diastereotopic *N*-methyl groups are expected in the ¹H and ¹³C NMR spectra. Observation of only two *N*-methyl signals in **6a** further confirms the equal structures in solution and in the crystal.⁶ Increasing the sample temperature of **6a** up to 370 K did not result in significant line broadening or exchange phenomena. To measure a substantially high barrier for methyl interconversion, we resorted to the selective inversion recovery (SIR)

(6) Strictly speaking, the two chelate rings in the solid **6a** are not related by the molecular C_2 axis and, hence, are slightly different from each other.

Table 1. Selected Bond Lengths (Å) and Angles (deg) in Crystals of 6a, 7a, and 8

6a		7a		8	
Distances					
Si(1)–O(1)	1.759(3)	Si(1)–O(1)	1.7401(17)	Si(1)–O(1)	1.7607(11)
Si(1)–O(2)	1.757(3)	Si(1)–N(2)	1.756(2)	Si(1)–O(3)	1.7707(11)
Si(1)–O(3)	1.731(3)	Si(1)–O(3)	1.7641(17)	Si(1)–O(2)	1.7784(11)
Si(1)–O(4)	1.735(3)	Si(1)–O(2)	1.7653(16)	Si(1)–O(4)	1.8023(11)
Si(1)–N(1)	2.010(3)	Si(1)–N(5)	2.016(2)	Si(1)–C(16)	1.9180(16)
Si(1)–N(4)	1.997(3)	Si(1)–N(4)	2.044(2)	Si(1)–N(4)	2.0809(14)
Angles					
O(1)–Si(1)–O(3)	174.72(13)	O(1)–Si(1)–O(3)	174.62(8)	O(1)–Si(1)–O(3)	170.85(6)
N(4)–Si(1)–N(1)	168.22(13)	N(2)–Si(1)–O(2)	173.32(9)	O(2)–Si(1)–O(4)	176.14(6)
O(4)–Si(1)–O(2)	175.40(13)	N(5)–Si(1)–N(4)	165.52(8)	C(16)–Si(1)–N(4)	172.12(6)
O(3)–Si(1)–O(4)	90.19(12)	O(1)–Si(1)–O(2)	90.65(8)	O(3)–Si(1)–O(4)	91.80(5)
O(3)–Si(1)–O(2)	88.96(13)	O(3)–Si(1)–O(2)	91.56(8)	O(1)–Si(1)–O(4)	88.08(5)
O(3)–Si(1)–N(4)	95.44(13)	O(3)–Si(1)–N(2)	92.93(9)	O(1)–Si(1)–O(2)	89.42(5)
O(4)–Si(1)–N(4)	92.07(12)	O(1)–Si(1)–N(2)	85.30(8)	O(2)–Si(1)–O(3)	90.20(5)

Table 2. NMR Chemical Shifts (ppm) for the N-Methyl Groups in 6a,b, 7a,c, and 8 at 300 K in Toluene-*d*₈ Solutions

compound	²⁹ Si	¹ H ^a		¹³ C	
6a	–141.0	2.48	3.07	50.00	50.44
6b	–141.1 ^b	2.23	2.60	49.19	49.59
	–141.2 ^b	2.26	2.62	49.25	49.64
7a		2.28	2.63	48.91	49.65
		2.29	2.65	48.92	49.66
	–138.8	2.54	2.89	48.52	49.42
7c		2.52	3.03	49.32	50.10
	–140.2	2.27	2.38	47.76	48.62
	–140.3	2.28	2.42	48.08	48.94
8		2.30	2.47	48.46	49.21
		2.32	2.52	48.59	49.30
	–148.2	2.47	2.82	49.28	59.25
		2.55	3.11	50.87	61.68

^a Two distinct chemical shift regions are found in all compounds, labeled A and B. ^b Only two signals were partly resolved.

Table 3. Kinetic Data for N-Methyl Exchange in 6a, Obtained by SIR Measurements at Three Temperatures, in Toluene-*d*₈ Solution at 500.13 MHz

temperature, K	rate constant <i>k</i> , s ^{–1}	Δ <i>G</i> [*] , kcal mol ^{–1}
360	1.86	20.8
370	4.32	20.7
375	7.00	20.6

technique, which allows accurate rate measurements at temperatures about 50 °C below the coalescence temperature.^{3,7} The SIR spectra were measured at three temperatures and yielded first-order rate constants and the corresponding free energy barriers (Table 3). The SIR spectra at 360 K are depicted in Figure 4. A rough Eyring correlation made from the results at three temperatures yielded Δ*H*^{*} = 22.7 kcal mol^{–1} and Δ*S*^{*} = 5.4 cal mol^{–1} K^{–1} (*R* = 0.999). The relatively low entropy of activation is in accord with an intramolecular exchange process.

This relatively high barrier in **6a** could, in principle, result from one of two different intramolecular processes: (i) dissociation of the Si–N bond, followed by fast rotation about the N–N bond and recombination, (ii) exchange of the hydrazide chelate oxygens via a (O,O)-1,2-shift (Figure 5).^{2b,c} The NMR spectra do not permit a distinction between these two processes. To answer this question, a similar tris-chelate was pre-

Table 4. Crystal Data and Experimental Parameters for the Crystallographic Analyses for 6a, 7a, and 8

	6a	7a	8
empirical formula	C ₂₄ H ₂₆ N ₄ O ₄ Si ^a	C ₃₂ H ₃₆ N ₆ O ₃ Si ^b	C ₂₅ H ₂₈ N ₄ O ₄ Si
formula mass, g mol ^{–1}	498.03	580.76	476.60
collection <i>T</i> , K	173	173	173
λ(Mo Kα), Å	0.71073	0.71073	0.71073
cryst syst	monoclinic	triclinic	monoclinic
space group	<i>P</i> 2(1)/ <i>c</i>	<i>P</i> 1	<i>P</i> 2(1)/ <i>c</i>
<i>a</i> , Å	15.056 (4)	11.4742 (19)	9.5422(17)
<i>b</i> , Å	9.366 (2)	12.266(2)	19.193(3)
<i>c</i> , Å	8.328(5)	12.433(2)	13.130(2)
α, deg	90	77.949(4)	90
β, deg	96.442 (6)	63.614(3)	105.279(5)
γ, deg	90	89.411(3)	90
<i>V</i> , Å ³	2568(11)	1526(4)	2319.6(7)
<i>Z</i>	4	2	4
ρ _{calc} , Mg/m ³	1.288	1.264	1.365
<i>F</i> (000)	1044	616	1008
θ range, deg	2.45–23.27	1.99–28.32	1.93–26.38
no. of coll reflns	14 393	17 512	23 924
no. of indep reflns	3673	7599	4745
<i>R</i> _{int}	0.0595	0.0661	0.0471
no. of reflns used	3673	7599	4745
no. params	358	389	311
Goof	1.092	0.789	0.994
<i>R</i> 1 ^c [<i>I</i> > 2σ(<i>I</i>)]	0.0527	0.0470	0.0344
w <i>R</i> 2 ^d (all data)	0.1414	0.1117	0.0882
<i>g</i> ₁	0.0843	0.1250	0.0557
<i>g</i> ₂	0	0	0
max/min res electron dens (e Å ^{–3})	+0.283/–0.234	+0.211/–0.361	+0.279/–0.360

^a Crystallized with one additional CH₃CN molecule per substrate molecule. The solvent molecules are disordered about an inversion center. ^b Crystallized with one additional toluene molecule per substrate molecule. ^c *R*1 = ∑||*F*_o| – |*F*_c||/∑|*F*_o|. ^d w*R*2 = {∑[w(*F*_o² – *F*_c²)/∑w(*F*_o²)]^{1/2}.

pared (**6b**), into which two chiral carbon centers were introduced. **6b** may exist in three diastereomeric forms, labeled *RΔR*, *RΛR*, and *RΔS* (the latter is identical with *SΔR*), where the letters (*R*, *S*, Δ,⁸ Λ⁸) represent the absolute configurations of the chiral carbons and the silicon. The first two diastereomers have *C*₂ symmetry and hence give rise to two *N*-methyl signals each. The third diastereomer has no symmetry (*C*₁) and hence

(7) (a) Blanca, B.-D. M.; Maimon, E.; Kost, D. *Angew. Chem.* **1997**, *109*, 2294; *Angew. Chem., Int. Ed. Engl.* **1997**, *36*, 2216. (b) Orrell, K. G.; Sik, V. *Annu. Rep. NMR Spectrosc.* **1993**, *27*, 103.

(8) The Commission on the Nomenclature of Inorganic Chemistry of IUPAC: *Inorg. Chem.* **1970**, *9*, 1.

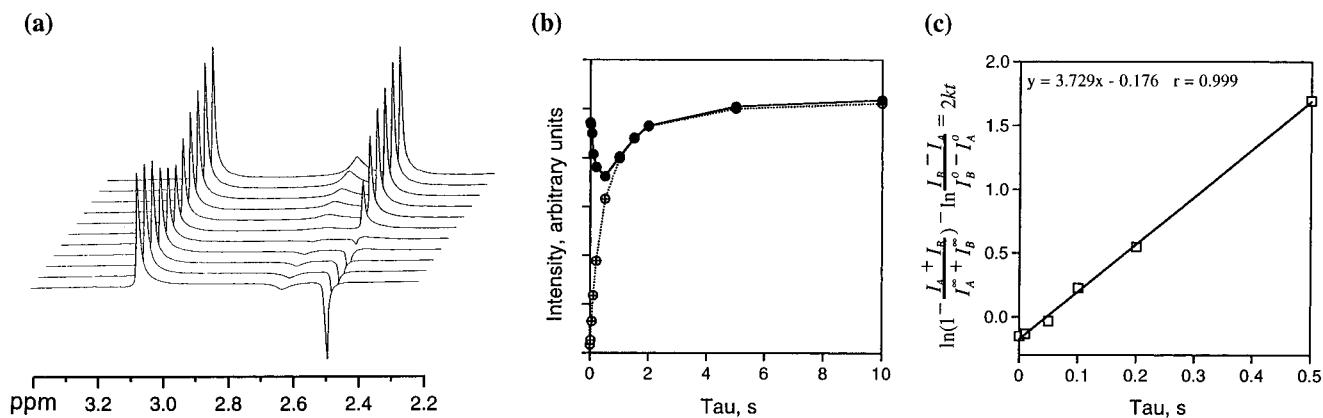


Figure 4. Selective inversion recovery (SIR) ^1H NMR spectra (500 MHz) of **6a** in toluene- d_8 solution at 360 K: (a) stack plot of spectra (N -methyl region); (b) plot of signal intensity vs variable delay time τ ; (c) linear correlation of data.

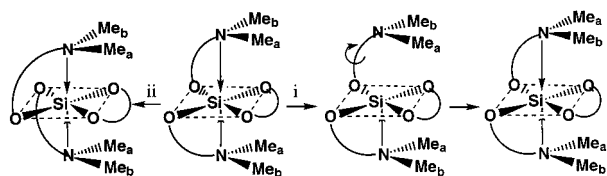


Figure 5. Schematic representation of the ligand-site exchange pathways in **6a** via (i) Si–N dissociation–recombination (two consecutive dissociation steps are required for complete exchange); (ii) (O,O)-1,2-shift. The labels of N -methyl groups were kept unchanged after the exchanges, for clarity, although their environments would be exchanged ($a \rightleftharpoons b$).

gives rise to four N -methyl signals. The resulting eight nearly equal intensity N -methyl signals are found in the ^1H and ^{13}C NMR spectra, as well as in the NOESY spectrum (Figure 6a).

The N -methyl exchange processes in **6b** were studied using 2D-NOESY spectra at various temperatures. At a relatively low temperature, 325 K, the exchange is slow relative to the NMR time scale and hence has no significant effect on the NOESY spectrum (Figure 6a,b). The only apparent cross signals are NOE interactions (negative peaks), connecting geminal N -methyl signal pairs. This spectrum serves for an unequivocal assignment of geminal N -methyl signals in the absence of exchange.

At a slightly elevated sample temperature, 340 K, the phase-sensitive NOESY spectrum (Figure 6c) features both negative (NOE) and positive (exchange) cross signals, indicating that at this temperature an N -methyl exchange process becomes significant with respect to the NMR time scale. Examination of Figure 6c reveals that exchange signals do not connect geminal N -methyl pairs; that is, the observed kinetic process does not interchange geminal groups. Obviously, the absence of geminal- N -methyl exchange rules out a silicon–nitrogen dissociation–recombination sequence, and consequently the observed exchange is the flipping of the adjacent oxygen atoms, (O,O)-1,2-shift.

When the temperature is further increased to 360 K, the NOESY spectrum (Figure 6d) shows *two* exchange cross-signals for each N -methyl group, indicating that a second, independent, exchange process is now operative and affects the spectrum. Since now positive exchange cross signals have replaced the negative NOE peaks, it is evident that the second rate process does

bring about exchange of geminal N -methyl groups, i.e., that this second process is an N–Si dissociation–recombination sequence. Complete scrambling of all the N -methyl signals cannot be observed, even at high temperatures, because when rapid epimerization at silicon takes place, there still are two diastereomers present: RR and RS . This result provides evidence that inversion of configuration of the carbon centers does not take place at any of the studied temperatures, on the NMR time scale.

Thus, the evidence shows that in **6b** two consecutive N -methyl exchange processes take place: the first is assigned to an (O,O)-shift (epimerization at silicon), and the higher barrier process is assigned to N–Si dissociation–recombination.

Ligand-Site Exchange in 7a,c. **7a** has C_1 symmetry and therefore displays four N -methyl signals in the ^1H and ^{13}C NMR spectra. There are three reasonable, nondissociative intramolecular processes which can, in principle, effect exchange between the various N -methyl pairs: (i) Si–N dissociation–recombination; (ii) (O,O)-exchange of the two dimethylhydrazido chelates; and (iii) (O,N)-exchange of the third chelate ring. Examination of a model reveals that each of these processes should have different stereochemical consequences: process i should interchange, when rapid on the NMR time scale, between A and B N -methyl groups (geminal, see Figure 7). Process ii results in the exchange $A \rightleftharpoons B'$ and $B \rightleftharpoons A'$, while process iii exchanges between A and A' , and between B and B' (A and B refer to geminal N -methyl groups, while A' and B' refer to groups exposed to similar chemical environments: A and A' flank the NH-hydrazido chelate ring on each side, while B and B' point away from that ring; see Figure 7).

These three N -methyl exchange options are readily distinguished by a 2D-NOESY spectrum of **7a** at 300 K (Figure 8). At this temperature, both negative (NOE) and positive (exchange) cross signals are observed. The NOE signals unequivocally identify the geminal N -methyl pairs. The exchange signals are clearly neither between geminal groups (A, B) nor between groups of similar chemical environments (A, A' or B, B'), but represent the exchange $A \rightleftharpoons B'$ and $B \rightleftharpoons A'$. This result leads directly to the following two conclusions: (a) that the exchange process must be nondissociative (because dissociation of the N \rightarrow Si bond would have caused the

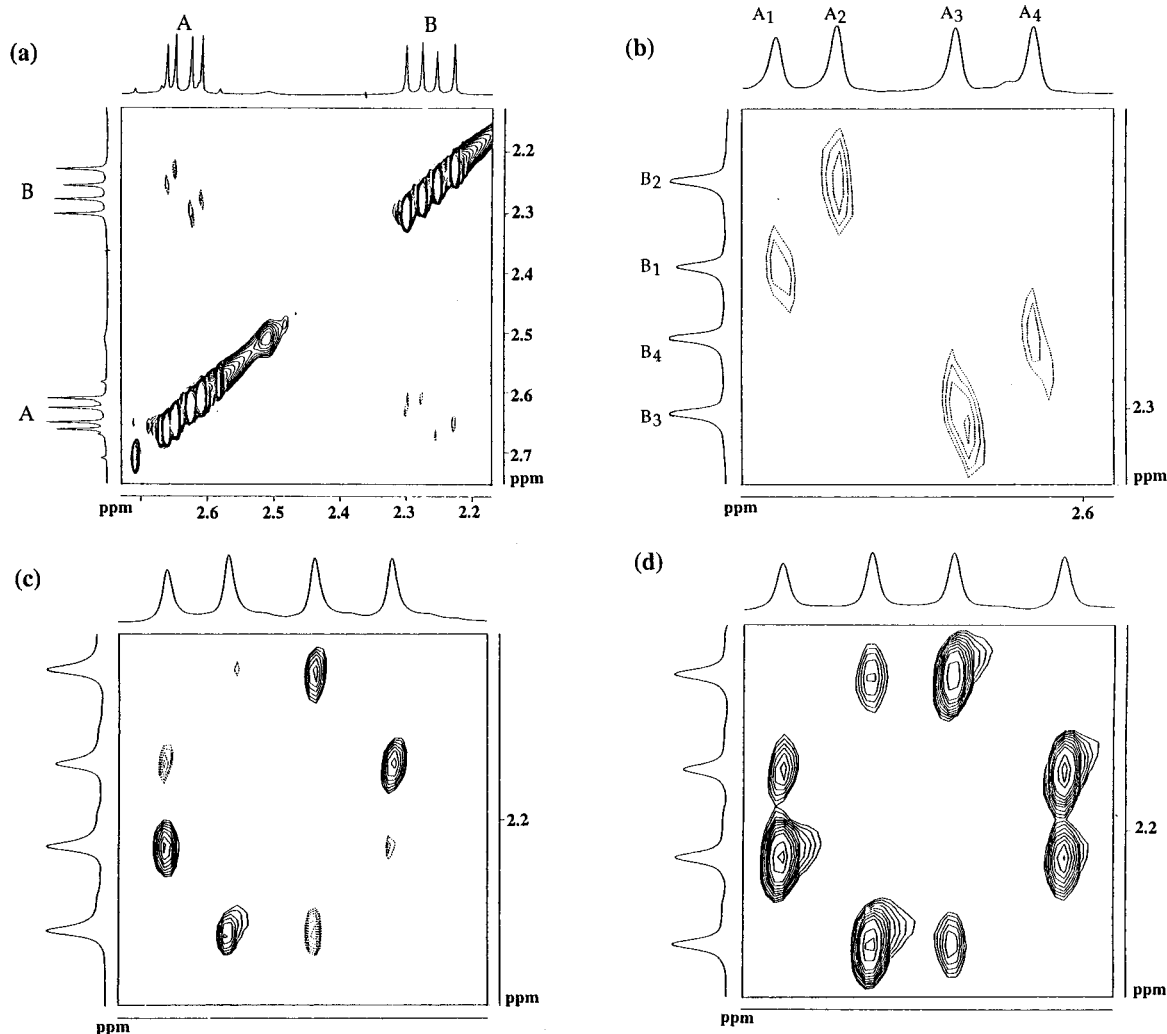


Figure 6. ^1H NMR (500 MHz) phase-sensitive NOESY and exchange spectra for **6b** (toluene- d_6): (a) full *N*-methyl range at 325 K, showing four A and four B signals for three diastereomers, with NOE (negative, dotted line) cross-signals identifying geminal pairs; (b) expansion of upper left part of (a): A-type signals are assigned arbitrary numbers, with corresponding numbers for B-signals due to geminal methyl groups; (c) the same region at 340 K, showing *N*-methyl exchange (solid lines) of *nongeminal* groups; (d) at 360 K two exchange processes are observed, without total scrambling.

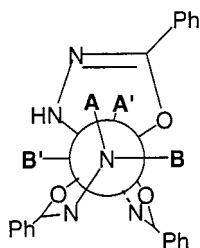


Figure 7. Newman projection of **7a**, viewed along the N–Si–N axis. The *N*-methyl groups are labeled A, A', B, B'.

exchange $A \rightleftharpoons B$) and (b) that the observed exchange is ii, the interchange of the dimethylhydrazido chelates via (O,O)-shift.

This exchange of the two dimethylhydrazido chelate rings is also confirmed by variable-temperature 1D ^1H NMR spectra of **7a** in toluene- d_6 solution, featuring line broadening and exchange of the ortho-protons of the corresponding phenyl rings (coalescence temperature 365 K, $\Delta G^\ddagger = 18.5 \pm 0.2 \text{ kcal mol}^{-1}$). Further increase of temperature leads to further line broadening and exchange. However, the spectra cannot provide an

answer as to whether the second kinetic process involves N–Si dissociation (i) or (N,O)-exchange (iii). To assign the correct stereomutation to the second kinetic process, complex **7c** was prepared, from *optically pure R*-2-phenylpropionic acid. Two diastereomers are observed in the NMR spectra: $R\Delta R$ and $R\Lambda R$, with four unique *N*-methyl groups in each, for a total of eight singlets.⁹

The 300 K NOESY spectrum of **7c** (Figure 9a) provides the exact assignment of geminal *N*-methyl groups. At 345 K the NOESY spectrum (Figure 9b) shows *geminal* exchange. Because of the chiral carbon centers, which render the geminal *N*-methyl groups diastereotopic even when epimerization at silicon is rapid, geminal exchange can result *only* from N–Si dissociation. It follows that at this temperature N–Si dissociation in **7c** is rapid relative to the NMR time scale. In addition, a second exchange process is evident from Figure 9, generating at least *two* exchange cross-signals for each *N*-methyl group. Judging from **7a**, this process most likely is the (O,O) exchange. However, the possibility that all three processes are rapid on the NMR

(9) The optically pure acid was used to simplify the NMR spectra.

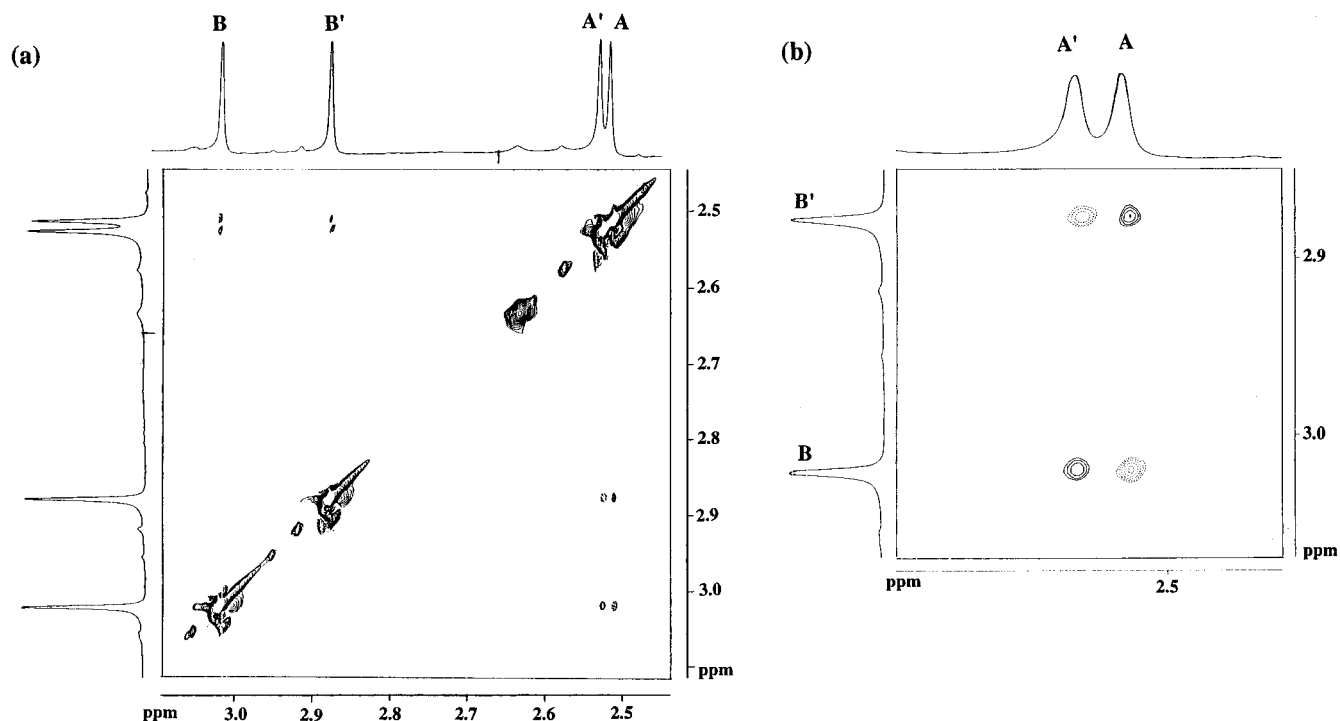


Figure 8. 2D-NOESY and exchange ^1H NMR spectrum of **7a** (500 MHz, toluene- d_8 , 300 K): (a) full *N*-methyl region; (b) expansion, showing geminal pairs (negative, dotted cross signals) and interchange of nongeminal pairs (positive cross-peaks).

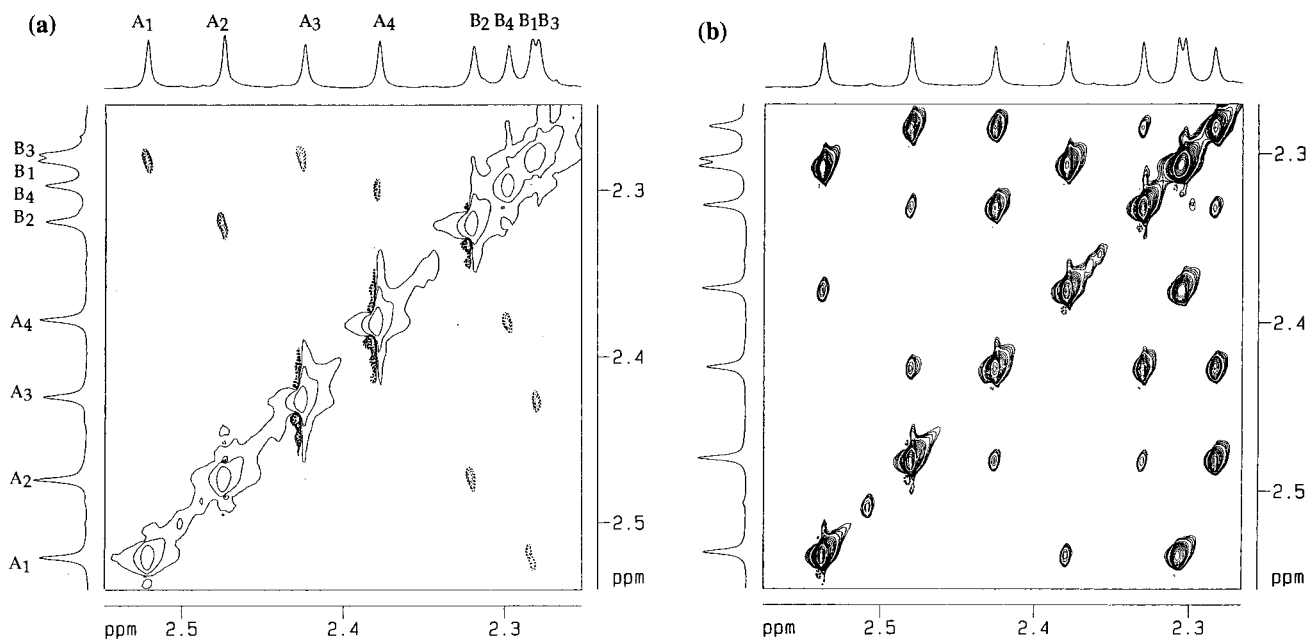


Figure 9. 2D-NOESY and exchange ^1H NMR spectra of **7c** (500 MHz, toluene- d_8 solution): (a) at 300 K, showing geminal pairs (A-signals are numbered arbitrarily and B-signals are numbered to correspond to their geminal A counterparts); (b) at 345 K, showing at least two exchange processes.

time scale at this temperature may be ruled out, since this would cause complete scrambling of all *N*-methyl signals. This is not the case in Figure 9b.

In summary, the low-barrier process in **7a** and **7c** is the (O,O)-exchange, followed by N–Si dissociation–recombination.

Ligand Site Exchange in 8. The tris-chelate **8**, with three different chelate rings and lacking any molecular symmetry (C_1), displays in the ^1H and ^{13}C NMR spectra four *N*-methyl signals and an AB quartet for the prochiral methylene protons in the ^1H spectrum. Two

consecutive kinetic ligand exchange processes, N–Si dissociation–recombination and (O,O)-exchange of the two hydrazido rings, can be observed by ^1H NMR spectroscopy. The first of these exchange reactions is observed by the coalescence of two of the initial four *N*-methyl signals, in the absence of exchange of the prochiral CH_2 protons ($T_c = 363\text{ K}$, $\Delta G^\ddagger = 16.1 \pm 0.2\text{ kcal mol}^{-1}$, Figure 10). This can result only from a dissociation–recombination sequence, which renders the two *N*-methyl groups in the five-membered chelate ring homotopic.

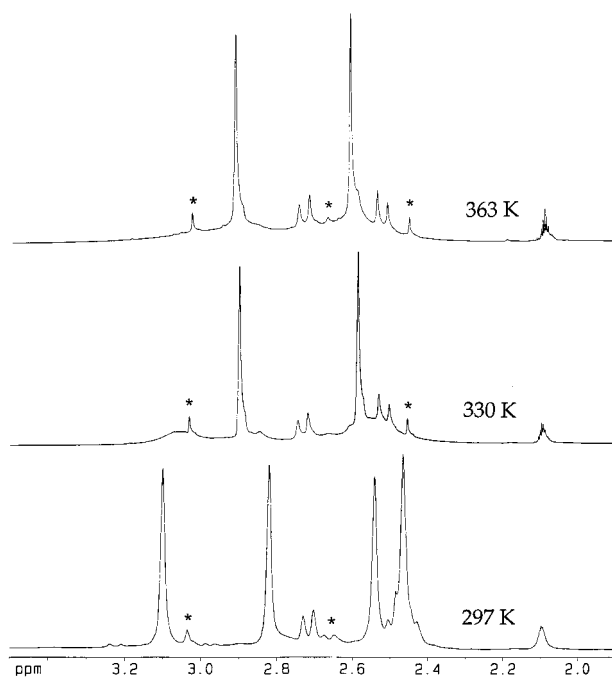


Figure 10. ^1H NMR spectra of **8** (500 MHz, toluene- d_8) at three temperatures, showing coalescence of one N -methyl signal pair only. Signals labeled * are due to hydrolysis products.

The second process was too slow to permit measurement of the coalescence temperature, and the SIR technique was employed for the determination of the exchange barrier. The first-order rate constant obtained by this method at 355 K was $k = 1.02 \text{ s}^{-1}$, corresponding to a free energy barrier $\Delta G^\ddagger = 20.9 \pm 0.1 \text{ kcal mol}^{-1}$.

Experimental Section

General Procedures. All the reactions were carried out under dry nitrogen or argon, using solvents dried and purified by standard methods. NMR spectra were recorded on a Bruker DMX-500 spectrometer operating at 500.130, 125.758, and 99.362 MHz, respectively, for ^1H , ^{13}C , and ^{29}Si spectra, and are reported in δ (ppm) relative to tetramethylsilane (TMS), as determined from standard residual solvent-proton (or carbon) signals. 2D-NOESY spectra were run using standard Bruker software. SIR experiments were run as reported previously.^{3,7}

Single-crystal X-ray diffraction patterns were measured at 173(2) K on a Bruker SMART CCD 1000 diffractometer [$\lambda(\text{Mo K}\alpha) = 0.71073 \text{ \AA}$, graphite monochromator, a scan width of 0.3° in ω and exposure time of 10 s frame^{-1} , detector-crystal distance = 4.95 cm]. Experimental data are presented in Table 3. The complete crystallographic data (excluding structure factors) for the structures reported in this paper have been deposited with the Cambridge Crystallographic Data Centre as supplementary publications no. CCDC-160936 (**6a**), CCDC-160937 (**7a**), and CCDC-160938 (**8**). Copies of the data can be obtained free of charge on application to CCDC, 12 Union Road, Cambridge CB2 1EZ, UK [fax: (internat.) + 44(1223)-336-033; e-mail: deposit@ccdc.cam.ac.uk].

Elemental analyses were performed by Mikroanalytisches Laboratorium Beller, Göttingen, Germany.

Bis(*N*(dimethylamino)benzimidato-*N,O*(catecholato-*O,O*)silicon(IV) (6a**).** To a stirred solution of **1a**^{2b} (0.44 g, 0.85 mmol) in dry chloroform (15 mL) was added bis-(*O*-trimethylsilyl)catechol (**4**)¹⁰ (0.23 g, 0.91 mmol). The reaction mixture

was immersed momentarily in a liquid-nitrogen bath and partly evacuated until boiling commenced, after which it was sealed off. It was heated to $60\text{--}65^\circ\text{C}$ for 24 h. After cooling to room temperature the volatiles were removed under 0.1 Torr. The resultant oily mass was allowed to stand in dry hexane for 30 min, after which a solid separated. It was purified by quickly washing with cold CH_3CN (2 mL) and recrystallization from CH_3CN to yield a single crystal suitable for X-ray analysis. The analytical sample was recrystallized from chloroform. Yield: 0.29 g, 73%, mp $197\text{--}198^\circ\text{C}$. Anal. Calcd for $\text{C}_{24}\text{H}_{26}\text{N}_4\text{O}_4\text{Si}\cdot 0.5\text{CHCl}_3$: C, 56.34; H, 5.11; N, 10.73. Found: C, 57.00; H, 5.05; N, 10.45. ^1H NMR (toluene- d_8 , 300 K): 2.48 (s, 6H, 2 CH_3N), 3.07 (s, 6H, 2 CH_3N), 6.82 (m, 4H, C_6H_4), 6.96–7.97 (m, 10H, 2 C_6H_5). ^{13}C NMR (CDCl_3 , 300 K): 50.00 (CH_3N), 50.44 (CH_3N), 127.48, 128.15, 131.45, 149.87 (C_6H_5), 111.14, 119.71, 130.28 (C_6H_4), 165.16 ($\text{C}=\text{N}$). ^{29}Si NMR (CDCl_3 , 300 K): -141.0 .

Bis(*N*(dimethylamino)-(*R,S*)-2-phenylpropionimidato-*N,O*(catecholato-*O,O*)silicon(IV) (6b**).** The procedure is the same as for **6a**, using **1b**¹¹ (0.19 g, 0.39 mmol) and **4** (0.12 g, 0.47 mmol). The oily product (0.13 g, 63%) consists of three diastereomers, which were not isolated. ^1H NMR (toluene- d_8 , 300 K): 2.23, 2.26, 2.28, 2.29 (4s, 6H, 2 CH_3N), 2.60, 2.62, 2.63, 2.65 (4s, 6H, 2 CH_3N), 1.18, 1.28, 1.34, 1.36 (4d, $^3J = 7.2 \text{ Hz}$, 6H, CCH_3), 3.20, 3.30, 3.41, 3.46 (4q, $^3J = 7.2 \text{ Hz}$, 2H, CH). ^{13}C NMR (toluene- d_8 , 300 K): 17.66, 17.86, 18.07, 18.31 (CCH_3), 41.84, 41.89, 42.10, 42.23 (CH), 48.91, 48.92, 49.19, 49.25 (NCH_3), 49.59, 49.64, 49.65, 49.66 (NCH_3), 110.67–150.52 (C_6H_4 , C_6H_5), 170.25, 170.30, 170.42, 170.44 ($\text{C}=\text{N}$). ^{29}Si NMR (toluene- d_8 , 300 K): -141.1 , -141.2 .

Bis(*N*(dimethylamino)benzimidato-*N,O*(*N*(amino)benzimidato-*N,O*)silicon(IV) (7a**).** The preparation was like that for **6a**, using **1a** (0.20 g, 0.47 mmol) and *N,O*-bis-(trimethylsilyl)benzhydrazide (**5**)¹² (0.15 g, 0.54 mmol). The resultant oily mass was dissolved in dry chloroform (5 mL). Colorless crystals of **7a** were obtained by cooling the concentrated solution to 0°C for 2 days. Yield: 0.17 g, 76%, mp $183\text{--}185^\circ\text{C}$. Anal. Calcd for $\text{C}_{25}\text{H}_{28}\text{N}_6\text{O}_3\text{Si}$: C, 61.45; H, 5.78. Found: C, 60.95; H, 5.64. ^1H NMR (toluene- d_8 , 300 K): 2.52 (s, 3H, CH_3N), 2.54 (s, 3H, CH_3N), 2.89 (s, 3H, CH_3N), 3.03 (s, 3H, CH_3N), 5.38 (s, 1H, NH), 7.92, 7.97, 8.11 (3d, $^3J = 7.2 \text{ Hz}$, 6H, *ortho*-H), 6.98–7.20 (m, 9H, *meta*- and *para*-H). ^{13}C NMR (toluene- d_8 , 300 K): 48.52, 49.32, 49.42, 50.10 (4s, CH_3N), 124.40–132.70 (C_6H_5), 151.03, 164.25, 164.57 ($\text{C}=\text{N}$). ^{29}Si NMR (toluene- d_8 , 300 K): -138.8 .

Bis(*N*(dimethylamino)-(*R*)-2-phenylpropionimidato-*N,O*(*N*(amino)benzimidato-*N,O*)silicon(IV) (7c**).** To a stirred solution of **1c**¹¹ (0.25 g, 0.52 mmol) in dry toluene (15 mL) was added *N,O*-bis-(trimethylsilyl)benzhydrazide (**5**)¹² (0.17 g, 0.61 mmol). The reaction mixture was immersed

(11) **1b**, made from racemic (*R,S*)-2-phenylpropion-2',2'-dimethylhydrazide, and **1c**, made from optically active (*R*)-2-phenylpropion-2',2'-dimethylhydrazide, were prepared as described previously for the Cl, Ph analogue bis(*N*(dimethylamino)-(*R*)-2-phenylpropionimidato-*N,O*)chloro(phenyl)silicon(IV).^{2c} They were characterized by their ^1H , ^{13}C , and ^{29}Si NMR spectra (available in the Supporting Information) and used further without isolation. **1b** (3 isomers: $R\Delta R$, $R\Delta R$, $R\Delta S = S\Delta R$): ^1H NMR (CDCl_3 , 300 K): 1.21, 1.34, 1.41, 1.44 (4d, $^3J = 7.2 \text{ Hz}$, 6H, CH_3C); 2.76, 2.79, 2.81, 2.94, 3.07, 3.12, 3.16, 3.17 (8s, 12H, CH_3N); 3.52, 3.53, 3.55, 3.59 (4q, $^3J = 7.2 \text{ Hz}$, 2H, CH); 7.23 (m, 10H, C_6H_5). ^{13}C NMR (CDCl_3 , 300 K): 17.29, 17.43, 17.48, 17.53 (CCH_3); 41.42, 41.45, 41.49, 41.52 (CH); 51.53, 51.59, 51.76, 51.78, 52.28, 52.29, 52.40, 52.46 (CH_3N); 126.72, 126.80, 126.86, 127.07, 127.13, 127.16, 128.15, 128.20, 128.25, 140.31 (C_6H_5); 169.00, 169.04, 169.11, 169.17 ($\text{C}=\text{N}$). ^{29}Si NMR (CDCl_3 , 300 K): -146.1 , -146.4 , -146.6 . **1c** (2 isomers, $R\Delta R$, $R\Delta R$): ^1H NMR (CDCl_3 , 300 K): 1.34, 1.41 (2d, $^3J = 7.2 \text{ Hz}$, 6H, CH_3C); 2.82, 2.87, 3.12, 3.18 (4s, 12H, CH_3N); 3.53, 3.59 (2q, $^3J = 7.2 \text{ Hz}$, 2H, CH); 7.23 (m, 10H, C_6H_5). ^{13}C NMR (CDCl_3 , 300 K): 17.50, 17.60 (CCH_3); 41.51, 41.55 (CH); 51.58, 51.84, 52.35, 52.46 (CH_3N); 126.75, 126.84, 127.12, 127.22, 128.25, 140.40 (C_6H_5); 169.03, 169.21 ($\text{C}=\text{N}$). ^{29}Si NMR (CDCl_3 , 300 K): -146.2 , -146.8 .

(12) Kost, D.; Kalikhman, I.; Krivosos, S.; Bertermann, R.; Burschka, C.; Neugebauer, R. E.; Pülm, M.; Willeke, R.; Tacke, R. *Organometallics* **2000**, *19*, 1083.

(10) Henglein, F. A.; Krämer, J. *Chem. Ber.* **1959**, *92*, 2585.

momentarily in a liquid-nitrogen bath and partly evacuated until boiling commenced, after which it was sealed off. It was heated to 80–85 °C for 24 h. After cooling to room temperature the volatiles were removed under 0.1 Torr, which resulted in an oily product (0.18 g, 65%). ¹H NMR (toluene-*d*₆, 300 K): 1.27, 1.31, 1.34, 1.37 (4d, ³*J* = 7.0 Hz, 6H, CCH₃), 2.27, 2.28, 2.30, 2.32, 2.38, 2.42, 2.47, 2.52 (8s, 12H, CH₃N), 3.28, 3.34, 3.45, 3.52 (4q, ³*J* = 7.0 Hz, 2H, CH), 4.92, 4.95 (2s, 1H, NH), 7.11–7.88 (m, 15H, C₆H₅). ¹³C NMR (CDCl₃): 17.20, 17.24, 17.49, 17.60 (CCH₃), 41.54, 41.59, 41.66 (CH), 47.76, 48.08, 48.46, 48.59, 48.62, 48.94, 49.21, 49.30 (NCH₃), 124.40–141.40 (C₆H₅), 151.60, 151.66, 153.30 (C=N), 170.19, 170.25, 170.27, 170.29 (C=N). ²⁹Si NMR (CDCl₃, 300 K): –140.2, –140.3.

[*N*(Dimethylamino)benzimidato-*N,O*][1-{(1,1-dimethyl-2-benzoyl)hydrazonium}methyl-*C,O*](catecholato-*O,O*-silicon(IV) (8**)).** To a solution of **2a**³ (0.35 g, 0.80 mmol) in dry chloroform (5 mL) was added 0.27 g (1.06 mmol) of **4**. The mixture was evacuated as described for **6a** and heated to 60 °C for 24 h. A colorless crystalline solid precipitated after the solution was kept in a freezer (about –5 °C) for 24 h. The solution was removed by decantation, and the crystals were washed with 3 mL of dry hexane. Yield: 0.25 g, 68%, mp 179–

180 °C. Anal. Calcd for C₂₅H₂₈N₄O₄Si: C, 63.00; H, 5.92; N, 11.75. Found: C, 63.21; H, 6.10; N, 11.75. ¹H NMR (toluene-*d*₆, 300 K): 2.47, 2.55, 2.82, 3.11 (4s, 12H, CH₃N), 2.47, 2.70 (ABq, ²*J* = 13.3 Hz, 2H, CH₂), 6.68 (m, 4H, C₆H₄), 6.78–7.71 (m, 10H, C₆H₅). ¹³C NMR (toluene-*d*₆, 300 K): 49.28, 50.87, 59.25, 61.68 (CH₃N), 50.87 (CH₂), 111.05–137.03 (C₆H₅), 150.16, 150.81, 164.90, 166.98 (C=N). ²⁹Si NMR (toluene-*d*₆, 300 K): –148.2.

Acknowledgment. We thank Dr. Arkady Ellern for the structure analyses. Financial support from the Israel Science Foundation and from the German Israeli Foundation for Research and Development (GIF) is gratefully acknowledged.

Supporting Information Available: Tables of additional crystallographic data for **6a**, **7a**, and **8**, stereoviews of the unit cells for **6a** and **7a**, and ¹H, ¹³C, and ²⁹Si NMR spectra for **1b**, **1c**, **6b**, **7c**, and **8**. This information is available free of charge via the Internet at <http://pubs.acs.org>.

OM010465D